



## Research Article

# Comparison of Bevacizumab Quantification Results in Plasma of Non-small Cell Lung Cancer Patients Using Bioanalytical Techniques Between LC-MS/MS, ELISA, and Microfluidic-based Immunoassay

Noriko Iwamoto,<sup>1,2</sup> Megumi Takanashi,<sup>1</sup> Takashi Shimada,<sup>1,2,7</sup> Jiichiro Sasaki,<sup>3</sup> and Akinobu Hamada<sup>4,5,6,7</sup>

Received 18 June 2019; accepted 27 July 2019; published online 20 August 2019

**Abstract.** The development of analytical techniques to study therapeutic monoclonal antibodies is expected to be useful for pharmacokinetic analysis and for the development of therapeutic indexes to determine dosage standards. To date, the blood concentration of antibody drugs has been analyzed by the enzyme-linked immunosorbent assay (ELISA). However, with the development of mass spectrometry and microfluidization technologies, the assay implication is drastically changing. We have developed an analytical validation method for many monoclonal antibodies and Fc-fusion proteins using Fab-selective proteolysis nSMOL coupled with liquid chromatography-mass spectrometry (LC-MS/MS). However, the correlation between the analyzed data characterization and the referable value from individual measurement techniques has not been adequately discussed. Therefore, in this study, we discussed in detail the relationship of the bioanalytical data from three different techniques, LC-MS/MS, ELISA, and microfluidic immunoassay, using 245 clinical plasma samples from non-small cell lung cancer patients treated with bevacizumab. The quantified concentration data of bevacizumab in human plasma indicated that the results obtained were almost the same correlation regardless of which technique was used. And the referable value from LC-MS/MS and microfluidic immunoassay were similar and correlated compared with ELISA.

**KEY WORDS:** bevacizumab; bioanalysis; ELISA; LC-MS; microfluidic immunoassay; nSMOL.

## INTRODUCTION

Individualized and optimized therapy by molecular target drugs has become increasingly important whereby practical chemotherapy is performed after scientifically

**Electronic supplementary material** The online version of this article (<https://doi.org/10.1208/s12248-019-0369-z>) contains supplementary material, which is available to authorized users.

<sup>1</sup> Leading Technology of Bioanalysis and Protein Chemistry, Shimadzu Corporation, Kyoto, Japan.

<sup>2</sup> Shimadzu Bioscience Research Partnership, Shimadzu Scientific Instruments, 21720 23rd Dr SE #250, Bothell, Washington 98021, USA.

<sup>3</sup> Research and Development Center for New Medical Frontiers, Kitasato University School of Medicine, Sagami-hara, Japan.

<sup>4</sup> Division of Molecular Pharmacology, National Cancer Center Research Institute, Tokyo, Japan.

<sup>5</sup> Department of Pharmacology and Therapeutics, Fundamental Innovative Oncology Core, National Cancer Center Research Institute, Tokyo, Japan.

<sup>6</sup> Division of Clinical Pharmacology and Translational Research, Exploratory Oncology Research & Clinical Trial Center, National Cancer Center, 5-1-1 Tsukiji, Chuo-ku, Tokyo, 104-0045, Japan.

<sup>7</sup> To whom correspondence should be addressed. (e-mail: [tashimada@shimadzu.com](mailto:tashimada@shimadzu.com); [akhamad@ncc.go.jp](mailto:akhamad@ncc.go.jp))

selecting a group of patients with expected drug efficacy considering individual differences in efficacy, toxicity, and side effects. (1,2) For optimized therapy, multi-dimensional clinical indicators such as genetic background, drug distribution, and immune activity are extremely important, as well as the expression level of the target molecule. (3–5) However, the therapeutic indices of monoclonal antibodies partly remain unclear, and thus, the dosage levels have not been adequately determined. (6–8) Recent clinical trials of trastuzumab and ramucirumab for advanced gastric cancer have reported a positive correlation between the overall survival and level of antibody drugs in circulation. (9,10) Therefore, the development of a comprehensive index that can accurately assess the efficacy of drugs is urgently required in practical cancer care. The overall pharmacokinetic (PK) analysis of monoclonal antibodies could be an important process to establish the reference of treatment effects for antibody treatment. (11–14)

We have been developing an antibody-drug monitoring technology using mass spectrometry (MS) for the application of clinical PK study, elucidation of drug efficacy, and tissue distribution analysis. (15,16) From bioanalysis of the biological components using liquid chromatography coupled with MS (LC-MS/MS), there are always issues that must be overcome such as separation performance, carryover in the chromatograph part, ionization suppression effect of target

molecules by extra coexisting ions, and desolvation efficiency in the MS. (17,18) Therefore, the overall optimization from sample preparation to MS detection must be considered in the development of analytical methods. Antibody drugs are mainly produced from immunoglobulin G (IgG) subtypes, and Fc-fused protein pharmaceuticals are also developed. As a primary structure, protein pharmaceuticals have a highly common configuration with Fc regions. Thus, it is possible to develop an analytical technique independent of a variety of antibodies by selectively proteolyzing and recovering the specific region of each antibody. We have developed a novel method for monoclonal antibodies, named nano-surface and molecular-orientation limited (nSMOL) proteolysis. Because the Fab is oriented toward the reaction solution by collection via the Fc loop in the resin pore, nSMOL can selectively react on the Fab by physicochemically limiting the access of trypsin to the antibody substrate. This is achieved using the difference between trypsin on the surface of nanoparticles with a 200 nm diameter and the IgG collection resin in a 100 nm pore. In this reaction, peptides with complementarity-determining regions (CDRs) can be reproducibly collected and quantitated by LC-MS/MS analysis while maintaining the antibody structure specificity and minimizing the large excess of tryptic peptides from the other IgGs and extra protease contamination. This enables application to largescale analysis by maintaining a clean MS interface. nSMOL can contribute to the establishment of a regulated LC-MS/MS assay by the analytical validation of many antibodies. To evaluate the antibody-drug efficacy, the analysis of drug distribution level in tumor cells or tissues is critical. (19,20) Because nSMOL takes advantage of the structural specificity of IgGs and is not affected by any other biological matrix, antibodies can be accurately quantitated from tissue homogenates using LC-MS/MS. (21)

IgGs are the second major population in the plasma proteome. Current antibody analysis is mainly performed using ligand-binding assay (LBA)-based methods with specific idiotypic collection/detection antibodies. With advances in the antibody development techniques that have high specificity for each substrate, LBA assays will continue to be an important analytical technique for monoclonal antibodies. However, due to the rapid innovation of antibody therapy such as combination therapies, bispecific antibodies, or antibody-drug conjugates, LBA technology might be lacking in general purpose, such as cross reactivities among animal species, matrix effect, inhibitory substrates, lot-to-lot variability, differences in assay data between individual reagents, simultaneous quantification methods, and the great time and expense required to develop the collection/detection antibodies. Recently, an LBA-based assay system using microfluidic technology was developed and is attracting attention. (22,23) This is a technique for performing LBA-based assay by high accuracy by placing solid-phase ligands onto highly integrated capture beads in a microfluidic device and sandwiching them with fluorescent-labeled detection antibodies. By integrating the capture resin at a high density and utilizing the antigen-antibody reaction close to the ideal 1:1 in a microdroplet while minimizing the sensitivity degradation due to miniaturization, it is possible to eliminate the factors of non-specific binding factors as much as possible and apply it to an automated assay platform. (24)

To date, we have performed our antibody bioanalysis based on LC-MS/MS. In this present study, we compare and analyze the detailed correlation between the data from three different assay method, enzyme-linked immunosorbent assay (ELISA), microfluidic immunoassay, and nSMOL, using clinical samples from non-small cell lung cancer patients treated with bevacizumab, and discuss the data characterization in antibody monitoring technologies.

## MATERIALS AND METHODS

### Chemicals

Trypsin-immobilized glycidyl methacrylate-coated nano-ferrite particle FG beads with surface activation by N-hydroxysuccinimide were purchased from Tamagawa Seiki (Nagano, Japan). (25) Toyopearl AF-rProtein A HC-650F resin was from Tosoh (Tokyo, Japan). Bevacizumab was obtained from Chugai Pharmaceutical (Tokyo, Japan). Individual male and female control human serum was from Kohjin Bio (Saitama, Japan). Modified porcine trypsin and P14R (fourteen proline repeats and one arginine on C-terminus) internal standard synthetic peptide was from Sigma-Aldrich (St. Louis, MO). n-octyl- $\beta$ -D-thioglucopyranoside (OTG) was from Dojindo Laboratories (Kumamoto, Japan). Ultrafree-MC GV centrifugal 0.22  $\mu$ m filter was from Merck Millipore (Billerica, MA). HCA184 and HCA 185 idiotypic anti-bevacizumab antibodies were from Bio-Rad Laboratories (Hercules, CA). Other reagents, buffers, and solvents were from Sigma-Aldrich and Wako Pure Chemical Industries (Osaka, Japan).

### Clinical Sample Information

Blood samples were collected from non-small cell lung cancer patients treated with bevacizumab at a steady-state dose of 15 mg/kg (day 8 or later) during a clinical study, and we analyzed these specimens for the present study. Each sample was placed in vacuum blood collection tubes containing EDTA-2K and the tubes were gently rotated to mix the contents. The tubes were immediately placed on ice. The blood samples were centrifuged at 4°C for 10 min at 3000 rpm. The separated plasma samples were stored in a freezer at a temperature below -80°C until subsequent analysis. This study was reviewed and approved by the relevant institutional review boards and signed informed consent was obtained from all patients prior to participation. The procedures were in accordance with the Helsinki Declaration.

### Bevacizumab Monitoring in Patient Plasma by nSMOL Assay

In the present study, we performed the bevacizumab assay in human plasma by nSMOL analysis with minor improvements as described in our previous study in accordance with Bioanalytical Method Validation Guidance for Industry on May 2019 from US Food and Drug Administration. (20) Briefly, all sample sets were prepared and stored at -80°C for 24 h or more before each assay. A

10  $\mu$ l sample of bevacizumab-spiked human plasma or clinical samples were diluted 10-fold by phosphate-buffered saline (PBS) containing 0.1% OTG, and the IgG fraction was collected with 25  $\mu$ l of PBS-substituted AF-rProtein A resin 50% slurry with gentle vortexing at 25°C for 5 min. Protein A resin was collected on an Ultrafree filter and washed twice by 300  $\mu$ l of PBS containing OTG and PBS by centrifugation (10,000 $\times$ g for 1 min), and substituted with 150  $\mu$ l of 25 mM Tris-HCl (pH 8.0) containing 10 pmol/ml P14R. nSMOL proteolysis was carried out using 10  $\mu$ g trypsin on FG beads with gentle vortexing at 50 °C for 5 h in a saturated vapor atmosphere. After the nSMOL process, the reaction was stopped by adding 10% formic acid at a final concentration of 0.5%. The peptide solution was collected by centrifugation (10,000 $\times$ g for 1 min) after removal of the Protein A resin and trypsin FG beads. These analytes were transferred into low protein binding polypropylene vials after magnetic separation, and triple quadrupole LC-MS/MS (LCMS-8050 and LCMS-8060, Shimadzu, Kyoto, Japan) multiple reaction monitoring (MRM) quantitation was performed. Bevacizumab was quantified using the validated signature peptide FTFSLDTSK on CDR2 of heavy chain. The MRM transition information is described in Table I. To confirm bevacizumab structure, STAYLQMNSLR on CDR2 of heavy chain and VLIYFTSSLHSGVPSR on CDR2 of light chain were also monitored (described in our previous study).

The peptide quantitation was analyzed by LC-electrospray ionization-MS with triple quadrupole (Nexera X2 and LCMS-8050/8060, Shimadzu). The LC-MS/MS conditions were as follows: solvent A, 0.1% aqueous formic acid; solvent B, acetonitrile with 0.1% formic acid; column, Shim-pack GISS C18, 2.1  $\times$  50 mm, 1.9  $\mu$ m, 20 nm pore (Shimadzu); column temperature, 50°C; flow rate, 0.4 ml/min; gradient program, 0–1.5 min: %B = 1, 1.5–5 min: %B = 1–35 gradient, 5–5.9 min: %B = 95 with flow rate 1 ml/min, 5.9–6.25 min: %B = 1 with flow rate 1 ml/min, and 6.25–7 min: %B = 1 with 0.4 ml/min. The MS spectra were obtained with an electrospray ionization (ESI) probe at temperature, desolvation line, and heat block at 300°C, 250°C and 400°C, respectively. The nebulizer, heating, and drying nitrogen gas flows were set to 3, 10, and 10 l/min, respectively. The dwell time was set to 30 msec for each transition. The MRM monitor ions of peptide fragments were imported from the measured values of the structure-assigned fragments by high-resolution LCMS analysis. CID Ar partial pressure in the Q2 cell was set to 270 kPa. The electrode voltage of Q1 pre-bias, collision cell Q2, Q3 pre-bias, and parent and fragment ion m/z were performed using optimization support software (LabSolutions, Shimadzu).

For MRM transition, 1 fragment ion of b- or y-series was selected for quantitation, and 2 ions were selected for structural confirmation based on the optimized MRM ion yield. For calibration of bevacizumab, seven calibration points (1.02, 2.56, 6.40, 16.0, 40.0, 100, and 250  $\mu$ g/ml in human control plasma) and blank plasma samples were configured. The calibrant standards were determined within 20% for lower limit of quantitation and 15% for other concentration. The QC sample standards before and after the clinical sample assays were determined within 15% from nominal concentration at 2.60, 16.0, and 100  $\mu$ g/ml. The concentration data was calculated by linear regression fitting with 1/cps<sup>2</sup> weighting.

### Bevacizumab Monitoring in Patient Plasma by ELISA Assay

The human anti-bevacizumab antibody was diluted to 500 ng/ml in PBS and 0.02% Tween 20 (PBS-T) with 1% bovine serum albumin (BSA), and immobilized at 5°C overnight on an ELISA microplate. The supernatant was discarded and washed three times with PBS-T, and the immobilized surface was blocked by PBS with 5% BSA at room temperature for 1 h. Clinical samples were diluted 40-fold by standard plasma and were then diluted 100-fold with PBS-T with 1% BSA. The diluted sample was captured on self-established anti-bevacizumab antibody-coated plate at room temperature for 3 h. After washing three times with PBS-T, anti-bevacizumab-horseradish peroxidase (HRP) antibody solution of 125 ng/ml in PBS-T with 1% BSA was added and incubated at room temperature for 1 h. After washing three times by PBS-T, trimethoprim (2,4-diamino-5-(3,4,5-trimethoxybenzyl)pyrimidine) solution was added to the HRP reaction for approximately 20 min in the dark. The colorimetric reaction was stopped by adding 5 mM HCl, and measured with a microplate reader (SpectraMax, Molecular Devices, San Jose, CA) at 450 nm to obtain the measurement and 540 nm for the reference wavelength. All clinical samples were averaged by duplicated analysis, and concentration data was regressed by the four-parameter logistic least-square method with 1/ $\times$  2 weighting using SoftMax Pro software. The calibration standards of bevacizumab were set in the range of 156 ng/ml to 100  $\mu$ g/ml for 8 points (156, 313, and 625 ng/ml, and 1.25, 2.5, 5.0, 10, and 100  $\mu$ g/ml) in human plasma. The calibrant standards were determined within 25% for lower limit of quantitation and 20% for other concentration. The QC sample standards before and after the clinical sample assays were determined within 20% from nominal concentration at 0.313, 1.25, and 5.00  $\mu$ g/ml.

**Table I.** MRM Transition Information for Bevacizumab Signature Peptide FTFSLDTSK

Signature peptide sequence	Region	Optimized MRM conditions				Role
		Transition m/z	Q1 pre-bias [V]	Collision [V]	Q3 pre-bias [V]	
FTFSLDTSK	H-chain of CDR2	523.3 > 797.4	–38	–18	–30	Quantitation
		523.3 > 898.5	–38	–20	–34	Structure
		523.3 > 650.3	–38	–19	–34	Structure

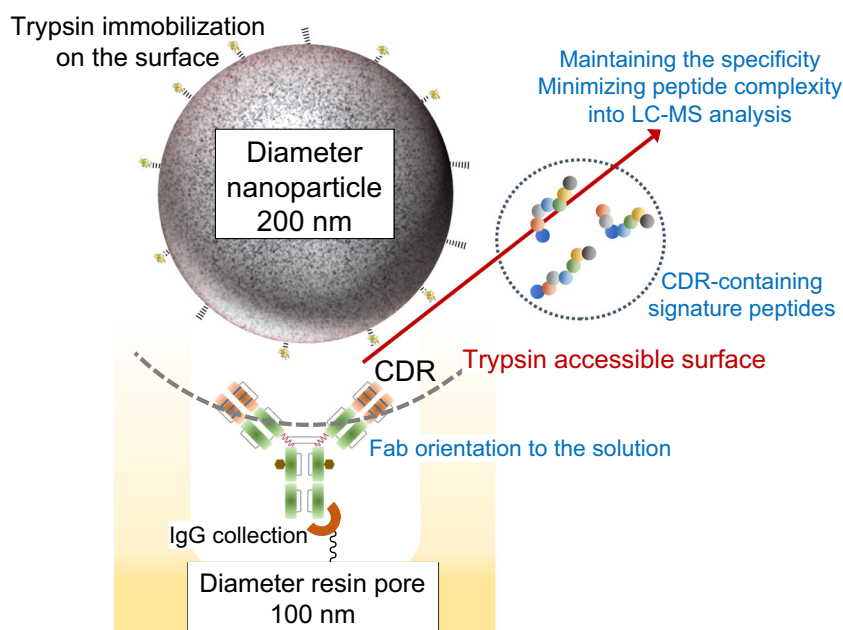


**Fig. 1.** The principle of Fab-selective proteolysis nSMOL

### Bevacizumab Monitoring in Patient Plasma by Microfluidic Immunoassay

The biotinylated anti-bevacizumab HCA184 antibody for capture antibody was diluted to 25  $\mu\text{g/ml}$  in PBS with 0.01% Tween 20 (PBS-T). Alexa 647-labeled anti-bevacizumab HCA 185 antibody for detection antibody was diluted to 40  $\mu\text{g/ml}$  in PBS-T. Clinical samples were diluted 50-fold with REXXIP NH solution (BioAgilytix, Durham, NC). All assay procedures were followed by the Gyrolab xP workstation standard protocol. Briefly, a needle was prewetted with PBS-T with 0.02% sodium azide, and washed by the same solution. A total of 4  $\mu\text{l}$  of the biotinylated capture antibody solution was added to streptavidin beads to bind to the resin. After washing, 4  $\mu\text{l}$  of the diluted clinical sample was loaded. The background noise was normalized and 4  $\mu\text{l}$  of Alexa 647-labeled detection antibody was added. The total volume to column resin was optimized to 200 nl per assay. The concentration was calculated using Gyrolab software with the 4-parameter logistic curve fitting. The calibration standards of bevacizumab were set at a range of 488 ng/ml to 500  $\mu\text{g/ml}$  with 11 points (0.488, 0.977, 1.95, 3.91, 7.81, 15.6, 31.3, 62.5, 125, 250, and 500  $\mu\text{g/ml}$ ) in human plasma. The calibrant standards were determined within 25% for lower limit of quantitation and 20% for other concentration. The

**Table II.** Bevacizumab Assay Summary of the Four Test Groups in nSMOL Analysis

	LCMS-8050	LCMS-8060
Operator 1 (scientist)	Assay set 1	Assay set 2
Operator 2 (laboratory technician)	Assay set 3	Assay set 4

QC sample standards before and after the clinical sample assays were determined within 20% from nominal concentration at 1.95, 15.6, and 250  $\mu\text{g/ml}$ .

### Comparison Data Analysis

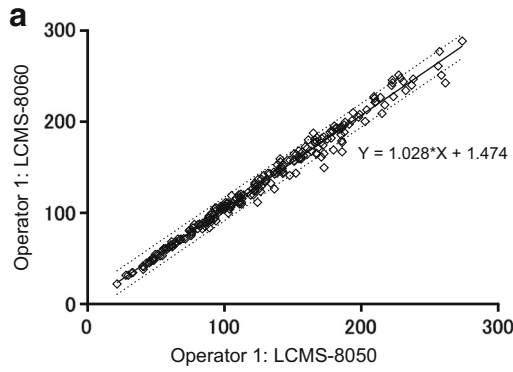
Data comparison was undertaken by Pearson's correlation analysis using linear logistic regression on GraphPad Prism version 7.05.

## RESULTS AND DISCUSSION

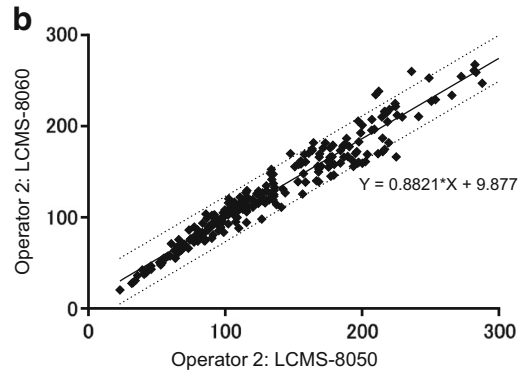
### Structure-Indicated Bioanalysis for Monoclonal Antibodies Using nSMOL Principle

It is necessary to have a whole and deep understanding of the features of the LCMS technologies in considering the bioanalysis method for high molecular weight proteins using mass spectrometry. Carryover performance needs to be controlled to ensure chromatographic resolution and reproducibility. In the ionization interface, it is necessary to overcome the ionization suppression effect and keep the ESI interface normal. And the conformation of the pharmaceutical antibody has a variable region Fab of N-terminus or fusion proteins linked to a Fc of C-terminus of the common sequences via flexible hinge. In a quantitative assay, the recovery of reliable signature peptides from antibodies enables an assay method that fully utilizes the molecular

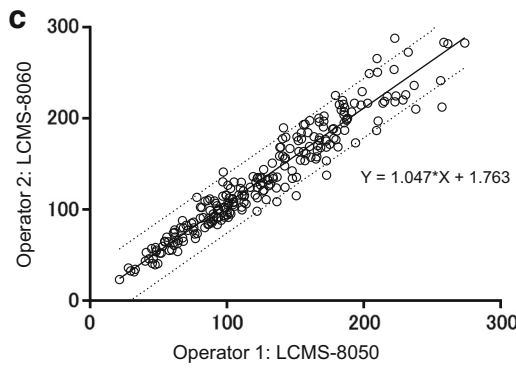
**Fig. 2** Pearson's correlation analysis of bevacizumab assay in clinical patient samples by nSMOL bioanalysis assay of the LC-MS difference of data obtained by a scientist ( $\diamond$ ) (a), the LC-MS difference data obtained by a technician ( $\blacklozenge$ ) (b), the operating person difference using the same LC-MS by a scientist ( $\circ$ ) (c), the operating person difference using the same LC-MS by a technician ( $\bullet$ ) (d), the LC-MS and operating person difference ( $\Delta$ ) (e), and the LC-MS and operating person difference ( $\blacktriangle$ ) by Pearson's correlation analysis (f). The equations show the fitting of linear approximate curve



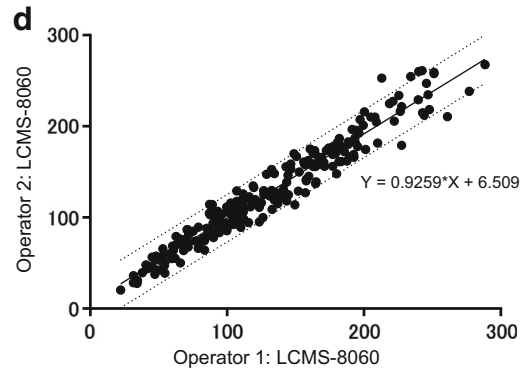
Comparison group 1	Pearson correlation coefficient	Linear regression slope (1/slope)
LC-MS difference Set 1 vs Set 2	0.9865	0.9728



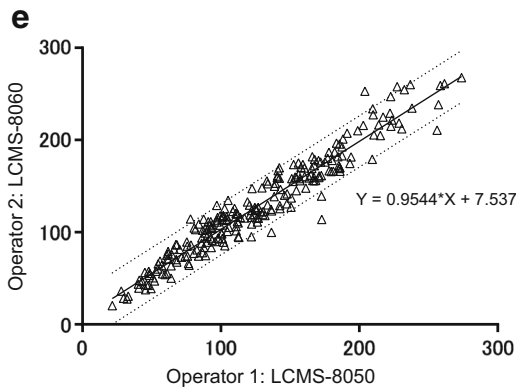
Comparison group 2	Pearson correlation coefficient	Linear regression slope (1/slope)
LC-MS difference Set 3 vs Set 4	0.9452	1.134



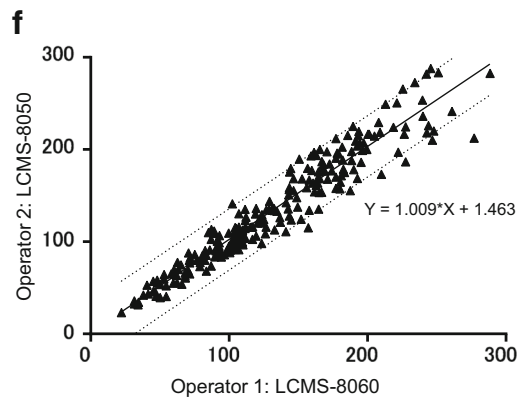
Comparison group 3	Pearson correlation coefficient	Linear regression slope (1/slope)
Operating person difference using the same LC-MS Set 1 vs Set 3	0.9232	0.9551



Comparison group 4	Pearson correlation coefficient	Linear regression slope (1/slope)
Operating person difference using the same LC-MS Set 2 vs Set 4	0.9398	1.080



Comparison group 5	Pearson correlation coefficient	Linear regression slope (1/slope)
LC-MS and operating person difference Set 1 vs Set 4	0.9318	1.048



Comparison group 6	Pearson correlation coefficient	Linear regression slope (1/slope)
LC-MS and operating person difference Set 2 vs Set 3	0.9196	0.9906

selectivity of hybrid LC-MS. Furthermore, by increasing the assay repeat speed with minimizing the sample complexity, it could be applicable to the practical clinical research. The theory of structure-indicated nSMOL proteolysis is significant for the development of bioanalysis assay in clinical studies of any antibody or Fc-fusion protein. The nSMOL is a sole technique of selective detection of CDR region of antibodies by physicochemically controlling the molecular diameter and orientation of the antibody and limiting the protease access to the Fab. In addition, nSMOL can be proceeded the highly efficient proteolysis in a non-denatured physiological condition by the nanomaterial structure of the reaction surface. The nSMOL concept is shown in Fig. 1.

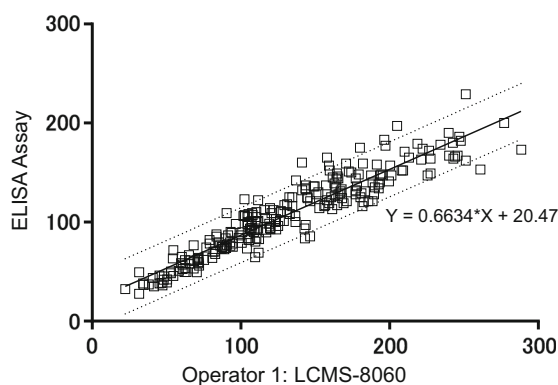
### Assay Reproducibility and Differences Between LC-MS Instruments and Human Errors in nSMOL Coupled with LC-MS Analysis

The bevacizumab concentration data prior to treatment in 30 patient samples was observed as ND using three methods of LC-MS/MS, ELISA, and microfluidic immunoassay. We verified the assay reproducibility and differences between instruments and human error using practical clinical samples. In Table II, the operators, assay sets, and instruments used in the present study are summarized. In this verification, we compared two sets of LC-MS/MS assay data obtained by a scientist using different types of triple quadrupole LC-MS/MS (LCMS-8050 and LCMS-8060) with the data obtained by a technician. In Fig. 2, we describe the correlation analysis results of all comparison sets. From these data comparisons, the nSMOL protocol showed a highly reproducible assay data using clinical sample, and the concentration data approximated by the calibration curve gave almost the same results regardless of the operating instruments or the person undertaking the analysis.

### Assay Reproducibility and Differences Between LC-MS/MS and LBA-Based Assay Using ELISA and Microfluidic Immunoassay

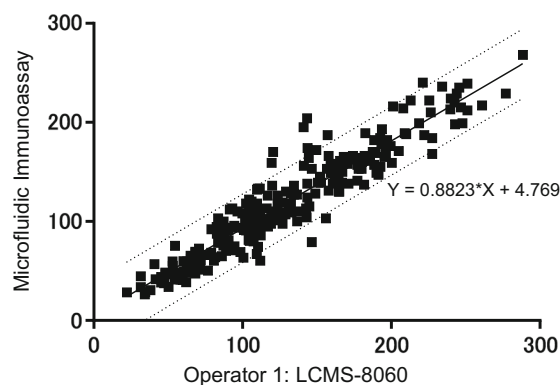
In this analysis, we compared two LBA-based assay data (ELISA and microfluidic immunoassay) with the results of assay set 2 from the LC-MS/MS analysis. We selected two idiotypic types of antibodies that specifically bound to the substrate in a biological matrix, with one having a detection tag attached to it. After that, it could be specifically detected by absorption or chemiluminescence analysis by making a sandwich of the substrate. In this case, all molecules having antigenicity can theoretically be detected; however, the preparation of a detection antibody requires great time and cost. If the binding site recognized by the detection antibody is blocked and/or masked by another substance, the substrate cannot be detected. For a monoclonal antibody assay, this corresponds to anti-drug antibodies or its target ligands. (26) Furthermore, LBA-based assays do not detect substrate directly. That is, the signal to be detected by LBA-based assay cannot definitely demonstrate that it is derived from the substrate.

The comparison data between nSMOL coupled with LC-MS/MS assay and ELISA showed that a data difference of approximately 20% occurred in the referable concentration values, even though the concentration data was correlated (Fig. 3). Conversely, the nSMOL and microfluidic immunoassay data showed that the data correlation and referable values were compatible (Fig. 4). According to the Reynolds number theory, it is demonstrated that the ratio of the force to fluid movement due to different viscosities is very low in the microenvironment, and the liquid flow changes from turbulent to laminar flow. In the laminar flow, the fluid in each boundary layer loses its traditionally mixing efficiency, and it depends only on free diffusion effect. Therefore, the interaction between the layer-stacked solid-phase detectors in the microfluidic devices and the monoclonal antibody in the solution enables an ideal antigen-antibody reaction in each layer. As a result, the antigen-antibody reaction by idiotypic



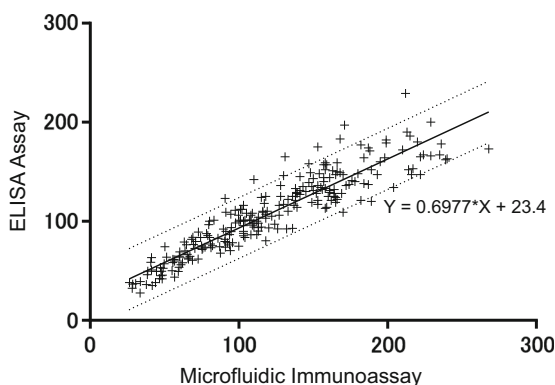
Condition	Pearson correlation coefficient	Linear regression slope (1/slope)
nSMOL vs ELISA	0.8765	1.507

**Fig. 3.** Bevacizumab assay comparison between nSMOL (assay set 2) and ELISA (□) by Pearson's correlation analysis



Condition	Pearson correlation coefficient	Linear regression slope (1/slope)
nSMOL vs microfluidic immunoassay	0.8899	1.133

**Fig. 4.** Bevacizumab assay correlation between nSMOL (assay set 2) and microfluidic immunoassay (■) by Pearson's correlation analysis



Condition	Pearson correlation coefficient	Linear regression slope (1/slope)
ELISA vs microfluidic immunoassay	0.8483	1.433

**Fig. 5.** Bevacizumab assay correlation between ELISA and microfluidic immunoassay (+) by Pearson's correlation analysis

antibody is preferentially proceeded. And these data could support that the antibody-antigen reaction in the microenvironment becomes unlikely to be inhibited by a substance because of the proximity effect and the increase in molecular contact surface. Similarly in nSMOL reaction, the contact surface of protease to antigen orientation is strictly controlled in microenvironment. It is assumed that the data resemblance in nSMOL and microfluidic immunoassay was obtained since the nSMOL principle occurs in a similar physical property of microfluidic atmosphere. For comparison of the ELISA and microfluidic immunoassay (Fig. 5), a data difference of approximately 20% occurred in the referable concentration values, although the concentration data was correlated similar to that LC-MS/MS assay.

### The Assay Data Differences of ELISA, and Microfluidic Immunoassay, and LC-MS/MS

We demonstrated that the experimental data derived from LC-MS/MS and microfluidic immunoassays might be correlated with precise values than ELISA when the plasma concentrations of bevacizumab were analyzed in clinical specimens.

### CONCLUSION

To the best of our knowledge, this is the first study to verify the LC-MS/MS bioanalysis data comparison with the LBA-based assay using clinical samples. Antibody bioanalysis techniques using nSMOL coupled with LC-MS/MS and microfluidic immunoassay are relatively compatible; however, the ELISA data should be considered in detail at its referable concentration.

Antibody bioanalysis using nSMOL proteolysis coupled with LC-MS is characterized by the ability to develop assay methods with very short times. In early drug development, the initial developing time of LC-MS/MS without using anti-antibody for the analytical method of biopharmaceuticals is more reasonable than ELISA since the developing time of

anti-antibody reagent is generally necessary for about a half year. Thus, we can accelerate the detailed PK study in any biological matrix, in circulation, and in cells or tissues using LC-MS/MS assays and applications. And this can then be applied to basic PK studies such as the accumulation in tumor cells/tissues, and for the selection and optimization of monoclonal antibody candidates before the preclinical studies.

### ACKNOWLEDGEMENTS

This study of the LBA-based assay was performed by Dr. Naoe Yamane of CMIC Pharma Science (Tokyo, Japan).

### COMPLIANCE WITH ETHICAL STANDARDS

This study was reviewed and approved by the relevant institutional review boards and signed informed consent was obtained from all patients prior to participation. The procedures were in accordance with the Helsinki Declaration.

### REFERENCES

- Chen SC, Quartino A, Polhamus D, Riggs M, French J, Wang X, et al. Population pharmacokinetics and exposure-response of trastuzumab emtansine in advanced breast cancer previously treated with  $\geq 2$  HER2-targeted regimens. *Br J Clin Pharmacol*. 2017;83(12):2767–77. <https://doi.org/10.1111/bcp.13381>.
- Geukes Foppen MH, Rozeman EA, van Wilpe S, Postma C, Snaebjornsson P, van Thienen JV, et al. Immune checkpoint inhibition-related colitis: symptoms, endoscopic features, histology and response to management. *ESMO Open*. 2018;3(1):e000278. <https://doi.org/10.1136/esmoopen-2017-000278>.
- Nishidate M, Hayashi M, Aikawa H, Tanaka K, Nakada N, Miura SI, et al. Applications of MALDI mass spectrometry imaging for pharmacokinetic studies during drug development. *Drug Metab Pharmacokinet*. 2019;34:209–16. <https://doi.org/10.1016/j.dmpk.2019.04.006>.
- Liu X, Lukowski JK, Flinders C, Kim S, Georgiadis RA, Mumenthaler SM, et al. MALDI-MSI of immunotherapy: mapping the EGFR-targeting antibody Cetuximab in 3D colon-cancer cell cultures. *Anal Chem*. 2018;90(24):14156–64. <https://doi.org/10.1021/acs.analchem.8b02151>.
- Randall EC, Emdal KB, Laramy JK, Kim M, Roos A, Calligaris D, et al. Integrated mapping of pharmacokinetics and pharmacodynamics in a patient-derived xenograft model of glioblastoma. *Nat Commun*. 2018;9(1):4904. <https://doi.org/10.1038/s41467-018-07334-3>.
- Roussey JA, Viglianti SP, Teitz-Tennenbaum S, Olszewski MA, Osterholzer JJ. Anti-PD-1 antibody treatment promotes clearance of persistent Cryptococcal lung infection in mice. *J Immunol*. 2017;199(10):3535–46. <https://doi.org/10.4049/jimmunol.1700840>.
- Lee CH, Romain G, Yan W, Watanabe M, Charab W, Todorova B, et al. IgG Fc domains that bind C1q but not effector Fcγ receptors delineate the importance of complement-mediated effector functions. *Nat Immunol*. 2017;18(8):889–98. <https://doi.org/10.1038/ni.3770>.
- Atzori F, Tabernero J, Cervantes A, Prudkin L, Andreu J, Rodriguez-Braun E, et al. A phase I pharmacokinetic and pharmacodynamic study of dalotuzumab (MK-0646), an anti-insulin-like growth factor-1 receptor monoclonal antibody, in patients with advanced solid tumors. *Clin Cancer Res*. 2011;17(19):6304–12. <https://doi.org/10.1158/1078-0432.CCR-10-3336>.

9. Saito M, Kawakami Y, Yamashita K, Nasuno H, Ishimine YU, Fukuda K, et al. HER2-positive gastric cancer identified by serum HER2: a case report. *Oncol Lett.* 2016;11(6):3575–8. <https://doi.org/10.3892/ol.2016.4470>.
10. Taberero J, Ohtsu A, Muro K, Van Cutsem E, Oh SC, Bodoky G, et al. Exposure-response analyses of Ramucirumab from two randomized, phase III trials of second-line treatment for advanced gastric or gastroesophageal junction cancer. *Mol Cancer Ther.* 2017;16(10):2215–22. <https://doi.org/10.1158/1535-7163.MCT-16-0895>.
11. Shah N, Mohammad AS, Saralkar P, Sprowls SA, Vickers SD, John D, et al. Investigational chemotherapy and novel pharmacokinetic mechanisms for the treatment of breast cancer brain metastases. *Pharmacol Res.* 2018;132:47–68. <https://doi.org/10.1016/j.phrs.2018.03.021>.
12. Li M, Kroetz DL. Bevacizumab-induced hypertension: clinical presentation and molecular understanding. *Pharmacol Ther.* 2018;182:152–60. <https://doi.org/10.1016/j.pharmthera.2017.08.012>.
13. Baker JHE, Kyle AH, Reinsberg SA, Moosvi F, Patrick HM, Cran J, et al. Heterogeneous distribution of trastuzumab in HER2-positive xenografts and metastases: role of the tumor microenvironment. *Clin Exp Metastasis.* 2018;35(7):691–705. <https://doi.org/10.1007/s10585-018-9929-3>.
14. Zhao X, Suryawanshi S, Hruska M, Feng Y, Wang X, Shen J, et al. Assessment of nivolumab benefit-risk profile of a 240-mg flat dose relative to a 3-mg/kg dosing regimen in patients with advanced tumors. *Ann Oncol.* 2017;28(8):2002–8. <https://doi.org/10.1093/annonc/mdx235>.
15. Iwamoto N, Shimada T, Umino Y, Aoki C, Aoki Y, Sato TA, et al. Selective detection of complementarity-determining regions of monoclonal antibody by limiting protease access to the substrate: nano-surface and molecular-orientation limited proteolysis. *Analyst.* 2014;139(3):576–80. <https://doi.org/10.1039/c3an02104a>.
16. Cruz E, Kayser V. Monoclonal antibody therapy of solid tumors: clinical limitations and novel strategies to enhance treatment efficacy. *Biologics.* 2019;13:33–51. <https://doi.org/10.2147/BTT.S166310>.
17. Yang Z, Hayes M, Fang X, Daley MP, Ettenberg S, Tse FL. LC-MS/MS approach for quantification of therapeutic proteins in plasma using a protein internal standard and 2D-solid-phase extraction cleanup. *Anal Chem.* 2007;79(24):9294–301. <https://doi.org/10.1021/ac0712502>.
18. Gong C, Zheng N, Zeng J, Aubry AF, Arnold ME. Post-pellet-digestion precipitation and solid phase extraction: a practical and efficient workflow to extract surrogate peptides for ultra-high performance liquid chromatography–tandem mass spectrometry bioanalysis of a therapeutic antibody in the low ng/mL range. *J Chromatogr A.* 2015;1424:27–36. <https://doi.org/10.1016/j.chroma.2015.10.049>.
19. Iwamoto N, Shimada T, Terakado H, Hamada A. Validated LC-MS/MS analysis of immune checkpoint inhibitor Nivolumab in human plasma using a Fab peptide-selective quantitation method: nano-surface and molecular-orientation limited (nSMOL) proteolysis. *J Chromatogr B Anal Technol Biomed Life Sci.* 2016;1023-1024:9–16. <https://doi.org/10.1016/j.jchromb.2016.04.038>.
20. Iwamoto N, Umino Y, Aoki C, Yamane N, Hamada A, Shimada T. Fully validated LCMS bioanalysis of Bevacizumab in human plasma using nano-surface and molecular-orientation limited (nSMOL) proteolysis. *Drug Metab Pharmacokinet.* 2016;31(1):46–50. <https://doi.org/10.1016/j.dmpk.2015.11.004>.
21. Iwamoto N, Shimada T. Recent advances in mass spectrometry-based approaches for proteomics and biologics: great contribution for developing therapeutic antibodies. *Pharmacol Ther.* 2018;185:147–54. <https://doi.org/10.1016/j.pharmthera.2017.12.007>.
22. Honda N, Lindberg U, Andersson P, Hoffmann S, Takei H. Simultaneous multiple immunoassays in a compact disc-shaped microfluidic device based on centrifugal force. *Clin Chem.* 2005;51(10):1955–61. <https://doi.org/10.1373/clinchem.2005.053348>.
23. Myzithras M, Bigwarfe T, Waltz E, Li H, Ahlberg J, Rybina I, et al. Optimizing NBE PK/PD assays using the Gyrolab Affinity Software; conveniently within the bioanalyst's existing workflow. *Bioanalysis.* 2018;10(6):397–406. <https://doi.org/10.4155/bio-2017-0251>.
24. Pohl G, Shih Ie M. Principle and applications of digital PCR. *Expert Rev Mol Diagn.* 2004;4(1):41–7.
25. Nishio K, Gokon N, Hasegawa M, Ogura Y, Ikeda M, Narimatsu H, et al. Identification of a chemical substructure that is immobilized to ferrite nanoparticles (FP). *Colloids Surf B: Biointerfaces.* 2007;54(2):249–53. <https://doi.org/10.1016/j.colsurfb.2006.10.039>.
26. Iwamoto N, Hamada A, Shimada T. Antibody drug quantitation in coexistence with anti-drug antibodies on nSMOL bioanalysis. *Anal Biochem.* 2018;540-541:30–7. <https://doi.org/10.1016/j.ab.2017.11.002>.

**Publisher's Note** Springer Nature remains neutral with regard to jurisdictional claims in published maps and institutional affiliations.